Non-Resonant Probabilistic Multipactor Calculations

Joakim Johansson[(1)] and Joel Rasch[(2)]

[(1)]RUAG Space AB
SE-405 15 Gothenburg, Sweden
Email:joakim.johansson@ruag.com

[(2)]Chalmers University of Technology
Department of Earth and Space Sciences
SE-412 96 Gothenburg, Sweden
Email: joel.rasch@chalmers.se

ABSTRACT

The parallel plate geometry along with the electron resonance condition have long been standard assumptions in the development of multipactor theory. In other geometries, field inhomogeneities yield ponderomotive forces, which in some cases reflect electrons back to the emitting surface, eliminating two-sided multipactor, but possibly giving rise to one-sided multipactor. In structures that are large in comparison to the electron oscillation amplitude, electrons can complete many cycles between impacts. A small perturbation in the emission phase or velocity can then lead to a large change in the transit time, resulting in a randomization of the impact phase, and thus calling for a probabilistic treatment.
A simple model for the electron motion close to the emission/impact surface is used to identify relationships between the emission and impact phases, where certain combinations of the parameters lead to identifiable "no-fly zones". A probabilistic transfer function that estimates the impact phase (and thus velocity) probability density function for a given emission phase probability density function is introduced. Combined with a secondary emission yield model, this can be used to study the evolution of the phase probability function for successive impacts.

INTRODUCTION

The parallel plate geometry along with the electron resonance condition have long been standard assumptions in the development of multipactor theory. The homogeneous field in the parallel plate structure is in some cases a good approximation, especially where fringing field effects can be neglected. In this simplistic model, necessary criteria for multipactor have generally been considered to be the resonant motion of electrons and sufficient voltage for the electrons to create secondary electrons at a rate higher than one per impact event [1, 2]. These criteria for multipactor are often summarized in the *Hatch-Williams* diagram, where multipactor-prone regions exist for combinations of voltage and frequency-gap-width product. Deviations from the resonance paradigm have been studied since the 70's when the spread in the emission velocity of the electrons were first taken into account [3]. It has been shown that even for a small spread in emission velocity, the effect on the multipactor zones in the *Hatch-Williams* diagrams is quite severe, and only the first resonance zone will be intact under realistic conditions [4].

For cases with a more inhomogeneous field the situation becomes different from the parallel plate geometry. The electron trajectories become more complicated, and the inhomogeneity of the field gives rise to ponderomotive forces, which in some cases will reflect electrons back to the emitting surface, eliminating two-sided multipactor, but possibly giving rise to one-sided multipactor. When RF structures are large compared to the electron oscillation amplitude, electrons will complete many RF cycles between impacts. To illustrate the effect, a simplistic coaxial structure can be studied. Given that the outer diameter and the impedance (ratio between outer and inner radius) are sufficiently large, electrons emitted from the outer conductor will never impact the inner conductor (see *e.g.* [5]). Fig. 1 shows a plot of the electron motion in such as system. The electron completes many RF cycles before returning back, and even a small perturbation in the emission velocity will lead to a large change in the transit phase. It is also seen that the motion of the electron is a combination of oscillatory component and a drift component that is influenced by the ponderomotive force. Locally, at the emission/impact surface, this drift component is quite linear, even if the field is highly inhomogeneous globally.

Since the transit time will be randomized to some extent, it is tempting to assume that the impact phase state will be unknown and indeterministic. Instead of the classical resonance condition one can thus use a statistical approach to evaluate the multipactor threshold. The statistical descriptions published so far consider the flight time of electrons, and evaluate the probability of impact at a certain phase depending on the original start phase, both for multipactor between parallel plates and the case of single sided multipactor caused by different arrangements of electric fields.

This is actually a complete probabilistic treatment, and the resulting function for the electron distribution function will be quite complicated, making it impossible to solve analytically. Instead of this complete statistical description of the system we here look at the local case for single sided multipactor.

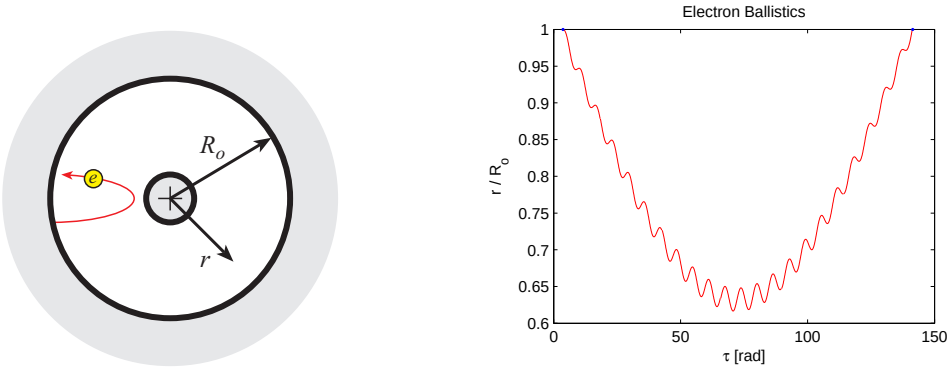

Fig. 1. A coaxial geometry (left) and a trajectory plot (right) of a case where the ponderomotive potential reflects back the electrons to the outer surface on a "long range return".

The statistical nature of the relation between emission and impact phase is illustrated in Fig. 2. The plot shows that the impact phase is deterministic in relation to the emission phase for certain ranges (0° – 180° and 270° – 360°), while being more chaotic for the remaining region. The plot also shows that there are certain combinations of phases that constitute "no-fly zones", and the density of dots is not uniform. To demonstrate the chaotic nature, two cases with a small difference in impressed RF field strength are plotted. The change in impact phase is dramatic compared to this small change, and a probabilistic treatment is thus to prefer compared to the nominally deterministic approach.

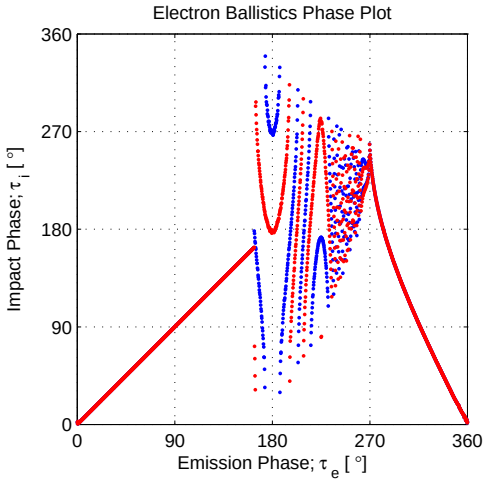

Fig. 2. The impact phase as function of the emission phase for a coaxial structure as in Fig. 1. Red and blue dots are data points for two cases that differ by 1 % in RF field strength.

As a first step in our analysis, the detailed nature of the returning agent can remain unspecified. Furthermore, this one-dimensional model is completely equivalent to a parallel plate system with a large gap width. We look at the area immediately above the metal surface, where there are electrons moving towards the surface and electrons moving away. Below a certain height above the surface, all the electrons moving towards the surface will impact during one period. At the same time this volume will be replenished again with electrons coming from outside, being randomly distributed in a band below this critical height. We will look at the distribution function of electrons over emission phase, the probability for impact depending on height, emission phase, emission speed and impact time. This allows us to formulate an analytical expression for the distribution over emission phase of secondary electrons. This expression enables us to calculate different impact probabilities, the average impact speeds, average secondary emission yields, and ultimately search for steady state distributions to locate the multipactor threshold.

ELECTRON MOTION

We now study the electron motion in a *gedanken* geometry. The electric field above the emission/impact surface is assumed to be *locally* homogeneous and in the form

$$\overline{E}(z,t) = \hat{z}\, E_o \sin \omega t \tag{1}$$

where E_o is the electric field amplitude, $\hat{z}$ the unit vector normal to the surface, ω the RF field angular frequency, and t the time (SI units are assumed everywhere in this paper, except for dimensionless, normalized parameters). The non-relativistic equation of motion is then

$$m_e \frac{d^2 z}{dt^2} = -eE_o \sin \omega t \tag{2}$$

Hence, electrons emitted at a time t_e with the initial speed v_{eo} will move according to

$$v_e(t) = v_\omega \left(\cos \omega t - \cos \omega t_e\right) + v_{eo} \qquad v_\omega = \frac{eE_o}{m_e \omega} \tag{3}$$

where $v_e(t)$ is the velocity in the z-direction. The amplitude of the oscillatory velocity v_ω is also defined, wherein e is the electron charge and m_e the electron mass. We now introduce the following normalized quantities to simplify the subsequent equations:

$$\tilde{v} = v/v_\omega \qquad \tau = \omega t \qquad \tilde{z} = z\omega/v_\omega \qquad \alpha = v_{eo}/v_\omega \tag{4}$$

resulting in

$$\tilde{v}_e(\tau) = \alpha - \cos \tau_e + \cos \tau = \tilde{v}_{ed} + \cos \tau \tag{5}$$

The velocity of electrons moving away from the surface thus consists of a drift component $\tilde{v}_{ed}$, which magnitude depends on the emission phase and the emission velocity, and an oscillatory part which magnitude is unity in the normalized system. Clearly, for the cases when $\tilde{v}_{ed} < 0$ there will be no emission of electrons into long trajectories, and such electrons will impact again within one period. Also, when $\dot{\tilde{v}}_e(\tau_e) < 0$ the electrons will be immediately pushed back towards the surface. Given sufficient emission velocity, the electrons will travel outward in a long trajectory. We will henceforth refer to those electrons which return within one period as "short range return electrons" and those that return only through the action of the ponderomotive force as "long range return electrons". The detailed criteria for long or short range returns are quite complicated and involve the solution of a transcendental equation. This has been done several times independently by *e.g.* [6, 7] but we defer this question to a later discussion, while we only mention now that given the criteria above, for $\alpha = 0$, the phase interval for long range return is $\tau_e \in [\pi, 3\pi/2]$, and for $\alpha >\approx 1.26$ it spans the full range, $\tau_e \in [0, 2\pi]$.

Upon emission the long range electrons have a positive drift velocity $\tilde{v}_{ed}$, but when they return later the impact drift velocity $\tilde{v}_{id}$ will be negative and of the same magnitude, *viz.* $\tilde{v}_{id} \equiv -\tilde{v}_{ed}$. This is due to the fact that the sum of the kinetic energy and the ponderomotive energy potential is conserved. Hence the expression for the velocity of the electrons returning to impact the surface is

$$\tilde{v}_i(\tau) = \tilde{v}_{id} + \cos \tau = -\tilde{v}_{ed} + \cos \tau = -\alpha + \cos \tau_e + \cos \tau \tag{6}$$

By integrating (6), we can find the position of incoming electrons starting at a height h at the beginning of every cycle:

$$\tilde{z}(\tau, h) = \sin \tau - \tilde{v}_{ed}\tau + h \tag{7}$$

The trajectory of incoming electrons moving with a drift speed, which shows all the essential features for the understanding of the trajectories, is shown in Fig. 3.

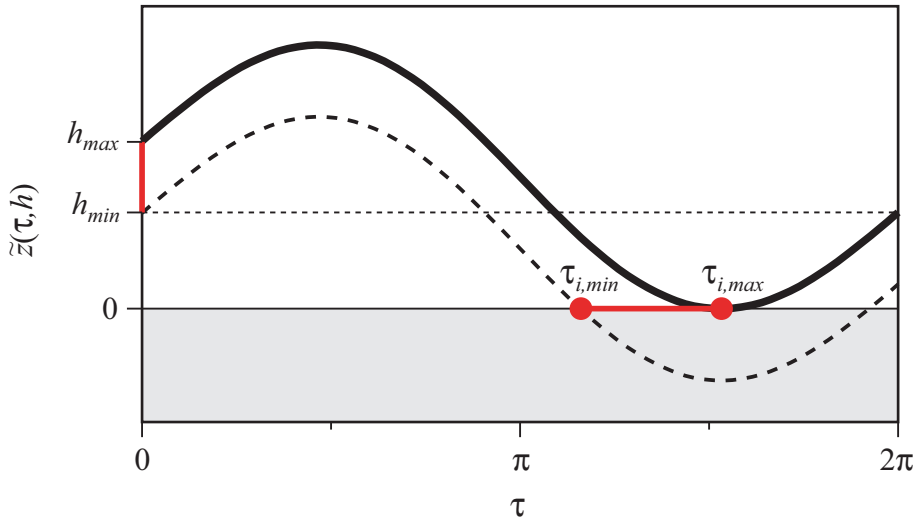

Fig. 3. The trajectories of incoming electrons. The solid curve shows the trajectory of electrons starting from the maximum height that allows impact. The dashed curve is located a distance of $2\pi\tilde{v}_{ed}$ below the solid curve, representing the subsequent cycle. The area between the two curves defines the trajectories that will replenish the surface with electrons during one period. The line above the shaded area represents the surface.

Electrons will only impact during a certain time interval, $\left[\tau_{i,min},\tau_{i,max}\right]$, depending on their drift speed. If $\tilde{v}_{ed}>1$ these limits become $\left[0,2\pi\right]$. But when $\tilde{v}_{ed}<1$ it is a bit more complicated. The right limit, $\tau_{i,max}$, corresponds to the point where the solid curved line touches the solid straight line. We find this time by solving $\tilde{v}_i\left(\tau_{i,max}\right)=0$, and get

$$\tau_{i,max}=2\pi-\arccos\tilde{v}_{ed} \tag{8}$$

The electrons which perform this motion start at a certain height, h_{max}, which is found by inserting $\tau_{i,max}$ into Eq. (5) and solving for $\tilde{z}\left(\tau_{i,max},h_{max}\right)=0$, leading to

$$h_{max}=2\pi\tilde{v}_{ed}+\sin\left(\arccos\tilde{v}_{ed}\right)-\tilde{v}_{ed}\arccos\tilde{v}_{ed} \tag{9}$$

The vertical distance between the solid curved line and the dashed curved line is simply the drift speed multiplied with 2π, since all electrons below this line would have already impacted during the previous field period. Therefore, the dashed line originates at $h_{\min}$, given by

$$h_{min}=\sin\left(\arccos\tilde{v}_{ed}\right)-\tilde{v}_{ed}\arccos\tilde{v}_{ed} \tag{10}$$

Hence, the minimum time for impact, $\tau_{i,min}$, is found by the solution of $\tilde{z}\left(\tau_{i,\min},h_{\min}\right)=0$, or

$$\sin\tau_{i,min}-\tilde{v}_{ed}\tau_{i,min}+\sin\left(\arccos\tilde{v}_{ed}\right)-\tilde{v}_{ed}\arccos\tilde{v}_{ed}=0 \tag{11}$$

The solution is not possible to express analytically in the general case. It is more instructive to show the limits in a graph, and then to use numerical solutions in the calculations. The limits are shown in the left panel of Fig. 4. A line drawn horizontally from the $\tilde{v}_{ed}$-axis will intersect the curves at two points, the left one representing $\tau_{i,\min}$, and the right one representing $\tau_{i,max}$.

It is also very important to find the limiting values for τ_e which correspond to a given τ_i. When $\tau_i>3\pi/2$ this is done by locating the intersection between a vertical line drawn from the τ_i-axis and the right curve for $\tilde{v}_{ed}$, in Fig. 2. If the value of $\tilde{v}_{ed}$ in the intersection is smaller than $\alpha-1$ the solution is simply $\tau_{e,min}=0$ and $\tau_{e,\max}=2\pi$, otherwise it is $\tau_{e,min}=\arccos\left(\alpha-\tilde{v}_{ed}\right)$ and $\tau_{e,min}=2\pi-\arccos\left(\alpha-\tilde{v}_{ed}\right)$. When $\tau_i<3\pi/2$ the same procedure is done with the left curve for $\tilde{v}_{ed}$. It is not possible to express the result analytically in a meaningful way, but the resulting curves for $\tau_{e,min}$ and $\tau_{e,\max}$ are shown in the right panel of Fig. 4 for three values of α.

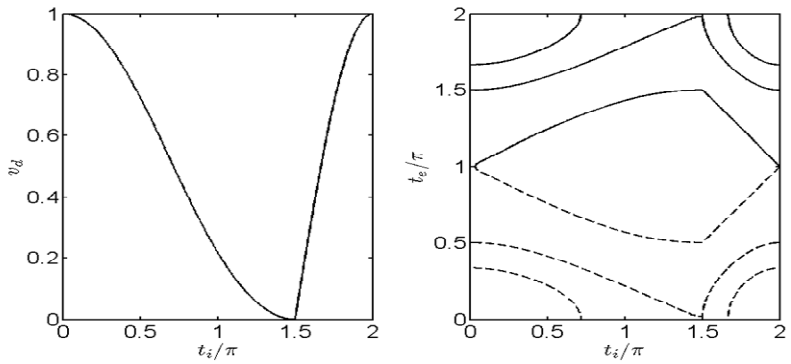

Fig. 4. The left panel shows the relationship between $\tilde{v}_{ed}$ and τ_i. The area above the curves is the region where impact is possible. The right panel shows the values for $\tau_{e,min}$ (dashed lines) and $\tau_{e,\max}$ (solid lines) as a function of τ_i for three different values of α; $\alpha = \{0, 1, 1.5\}$ from the centre and outwards.

PHASE DISTRIBUTION

We wish to describe the statistics of impacting electrons as a function of the emission phase, the emission speed, and the impact phase. To do this we need to consider how many electrons will be collected from a certain starting height above the surface given a specific impact phase. Clearly, when $\alpha < 2$, only electrons from certain emission phases will be collected at all impact phases. For electrons with $\tilde{v}_{ed} = 1$, any impact time is allowed, although they are more likely to impact during the times when they are moving rapidly, that is in an area around $\tau_i = \pi$. To describe this mathematically we introduce an emission phase distribution function, $n(\tau_e)$, which describes the ensemble of electrons that moves towards the surface and which will impact during one period. The function has the property

$$\int_0^{2\pi} n(\tau_e)\, d\tau_e = N \tag{12}$$

where N is the number of electrons. The fraction of electrons, $\eta(\tau_i, \tau_e)$, with emission phase τ_e that will impact at τ_i is the total number of electrons with emission phase τ_e multiplied by a small height segment, dh, divided by the entire height, $\Delta h(\tau_e) = 2\pi\tilde{v}_{ed} = 2\pi(\alpha - \cos\tau_e)$, from where these electrons are impacting during one period. In mathematical terms the fraction is

$$\eta(\tau_i, \tau_e)\, d\tau_e d\tau_i = n(\tau_e)\, d\tau_e \frac{dh}{\Delta h(\tau_e)} \tag{13}$$

This function $\eta_i(\tau_i, \tau_e)$ has the properties

$$n_i(\tau_i) = \int_{\tau_{e,min}}^{\tau_{e,max}} \eta_i(\tau_i, \tau_e)\, d\tau_e \qquad n_e(\tau_e) = \int_{\tau_{i,min}}^{\tau_{i,max}} \eta_i(\tau_i, \tau_e)\, d\tau_i \tag{14}$$

where $n_i(\tau_i)$ is the total number density of electrons impacting at the phase τ_i, and $n_e(\tau_e)$ is the total number density with emission phase τ_e impacting during a period.

The height segment, dh, is located at the height $h(\tau_i, \tau_e)$, which is just the height from where electrons with emission phase τ_e will impact at τ_i. It is found by solving (7) for $\tilde{z}(\tau_i, h) = 0$, giving

$$h(\tau_i, \tau_e) = (\alpha - \cos\tau_e)\tau_i - \sin\tau_i \tag{15}$$

The height segment, dh, is found by differentiating (15) with respect to τ_i, and we get

$$dh = (\alpha - \cos\tau_e - \cos\tau_i)\, d\tau_i \tag{16}$$

We combine (13) with (15) and get

$$\eta_i(\tau_i,\tau_e)d\tau_e d\tau_i = n(\tau_e)\frac{\alpha-\cos\tau_e-\cos\tau_i}{2\pi(\alpha-\cos\tau_e)}d\tau_i d\tau_e \tag{17}$$

If we let the impacting electrons generate secondary electrons, the incoming distribution of electrons will cause the emission of a new distribution. The average number of secondary electrons per impacting electron is described by the secondary emission yield function, σ, which depends on the impact speed, $\sigma=\sigma(\tilde{v}_i)=\sigma(\tau_i,\tau_e)$. The new distribution of electrons travelling outwards, $n'(\tau_i)$ is then

$$n'(\tau_i)=\int_{\tau_{e,min}}^{\tau_{e,max}}\sigma(\tau_i,\tau_e)n(\tau_e)\frac{\alpha-\cos\tau_e-\cos\tau_i}{2\pi(\alpha-\cos\tau_e)}d\tau_e \tag{18}$$

For a steady state to persist, the incoming distribution must generate a distribution of secondary electrons that is exactly the same, *i.e.* $n'(\tau_i)=n(\tau_e)$.

IMPACT PROBABILITY AND AVERAGE IMPACT SPEED

We wish to investigate how the probabilities for impact at different phases look, and we also wish to find the average impact speed. From (14) we know that the distribution of impacting electrons over impact phase looks like

$$n_i(\tau_i)=\int_{\tau_{e,min}}^{\tau_{e,max}}\eta_i(\tau_i,\tau_e)d\tau_e \tag{19}$$

The average impact speed for a certain impact time, τ_i, is the expectation value from

$$\left\langle\left|\tilde{v}_i(\tau_i)\right|\right\rangle=\frac{\int_{\tau_{e,min}}^{\tau_{e,max}}\left|\tilde{v}_i(\tau_i,\tau_e)\right|\eta(\tau_i,\tau_e)d\tau_e}{\int_{\tau_{e,min}}^{\tau_{e,max}}\eta(\tau_i,\tau_e)d\tau_e} \tag{20}$$

where $\left|\tilde{v}_i(\tau_i,\tau_e)\right|=\alpha-\cos\tau_e-\cos\tau_i$. It is more convenient to present this type of results as $n_i(\tau_i)\left\langle\left|\tilde{v}_i(\tau_i)\right|\right\rangle$, which is simply the result of multiplying the above formula with the denominator. Consequently the average impact speed for the entire emission phase distribution and the entire range of impact phases is

$$\left\langle\left\langle\left|\tilde{v}_i\right|\right\rangle\right\rangle=\frac{\int_0^{2\pi}\left\langle\left|\tilde{v}_i(\tau_i)\right|\right\rangle n_i(\tau_i)d\tau_i}{\int_0^{2\pi}n_i(\tau_i)d\tau_i} \tag{21}$$

Before tackling the full problem of finding steady state distributions of electrons, it is instructive to look at some simple applications to verify the consistency of the theory. Three quite obvious simple distributions are the uniform distribution, the infinitely narrow (delta) distribution (representing extremes), and a cosine-on-pedestal. Using (12), these distributions can be expressed as in Table 1, where $\delta(\tau)$ is the Dirac delta function, and τ_{eo} is the emission phase of all the electrons in the delta distribution. The integration limits are functions of τ_e and cannot in general be expressed in any simple form. However, when $\alpha>2$ the integration limits collapse to $[0,2\pi]$, and simple analytical methods can be used. The result of these integrations for the three distributions above is summarized in Table 1. It is seen that all three distributions result in an impact phase distribution of the type cosine-on-pedestal. Heuristically, this implies that there should exist a stable distribution.

Table 1. Impact distributions and average impact velocities for three emission phase distributions with $\alpha > 2$.

Emission Distribution	$n_e(\tau_e)$	$n_i(\tau_i)$	$n_i(\tau_i)\langle\langle\lvert\tilde{v}_i(\tau_i)\rvert\rangle\rangle$	$\langle\langle\lvert\tilde{v}_i\rvert\rangle\rangle$
Uniform	$\frac{N}{2\pi}$	$\frac{N}{2\pi}\left(1-\frac{\cos\tau_i}{\sqrt{\alpha^2-1}}\right)$	$\frac{N}{2\pi}\left(\alpha-2\cos\tau_i+\frac{\cos^2\tau_i}{\sqrt{\alpha^2-1}}\right)$	$\alpha+\frac{1}{2\sqrt{\alpha^2-1}}$
Cosine-on-Pedestal	$\frac{N}{2\pi\alpha}(\alpha-\cos\tau_i)$	$\frac{N}{2\pi\alpha}(\alpha-\cos\tau_i)$	$\frac{N}{2\pi}\frac{(\alpha-\cos\tau_i)^2+\frac{1}{2}}{\alpha}$	$\frac{\alpha^2+1}{\alpha}$
Delta	$N\delta(\tau_e-\tau_{eo})$	$\frac{N}{2\pi}\left(1-\frac{\cos\tau_i}{\alpha-\cos\tau_{eo}}\right)$	$\frac{N}{2\pi}\frac{(\alpha-\cos\tau_{eo}-\cos\tau_i)^2}{\alpha-\cos\tau_{eo}}$	$\frac{(\alpha-\cos\tau_{eo})^2+\frac{1}{2}}{\alpha-\cos\tau_{eo}}$

The above calculations are very important to get a sense of what the impact distributions should look like, and how the momentum of the impacting electrons will be distributed. The main effect of lowering α is that it creates an asymmetry in the impact distribution. The electrons tend to gather in the region $\tau_i \in [\pi, 3\pi/2]$. This is unfortunate, since electrons will be focused into the impact phases where the secondary emission is the strongest. The main objective of this first application of the new statistical theory is to estimate the number of electrons that will be lost simply due to the statistical spreading of incoming electrons into the regions where secondary emission is not possible.

The extreme case for losses is when $\alpha = 0$, since the electrons that impact in the interval $\tau_i \in [0, \pi]$ will be lost (never emitted), and those in $\tau_i \in [3\pi/2, 2\pi]$ are "short range returns" that have low energy. In Fig. 5, the impact distributions for $\alpha = 0$ are shown for the uniform distribution and a delta-distribution with $\tau_{eo} = \pi$.

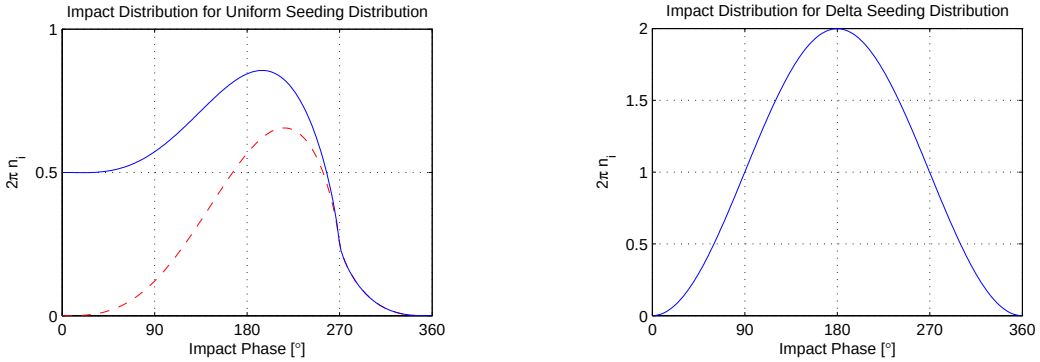

Fig. 5. The normalized distribution of incoming electrons when $\alpha = 0$ for a uniform seeding distribution over $\tau_e \in [0, 2\pi]$ (left panel) and a delta-distribution with $\tau_{eo} = \pi$ (right panel). In the left panel, the two cases of including (solid blue line) and excluding (dashed red line) the short range return electrons are shown for comparison.

The fraction of the impacting electrons that can contribute to long and short range returns is found by calculating the area under the curve in the intervals $\tau_i \in [\pi, 3\pi/2]$ and $\tau_i \in [3\pi/2, 2\pi]$ and dividing by the total area. This yields the fractions 0.36 and 0.03 for the uniform seeding distribution, and 0.41 and 0.09 for the delta seeding distribution.

An example of the evolution of a uniform seeding distribution through successive cycles of transit, impact, and secondary emission is shown in Fig. 6. The SEY model is based on a Vaughan type model (*cf.* [8]), and the energy level has been chosen to get a balance condition, *i.e.* a constant electron count. The emission and impact distributions are seen to quickly converge to stable shapes. The averaged velocity parameter is $\langle\langle\lvert\tilde{v}_i\rvert\rangle\rangle \approx 1.4$. The fractions in the long and short return intervals are 0.51 and 0.06, respectively. This implies that for a steady state distribution, the loss of electrons simply due to the statistical spreading of impacting electrons into the non-emitting phase region amount to roughly half the electron population. Simply from this we can conclude that non-resonant multipactor will be impossible for $\alpha = 0$ when the secondary emission yield maximum is below about 2. The fact that the statistical spread of electrons will lead to substantial loss of electrons, and therefore an increase in the voltage for multipactor breakdown, could account for the difference between the predictions based on a simplified approach, and Monte Carlo simulations which was seen in a recent investigation [9].

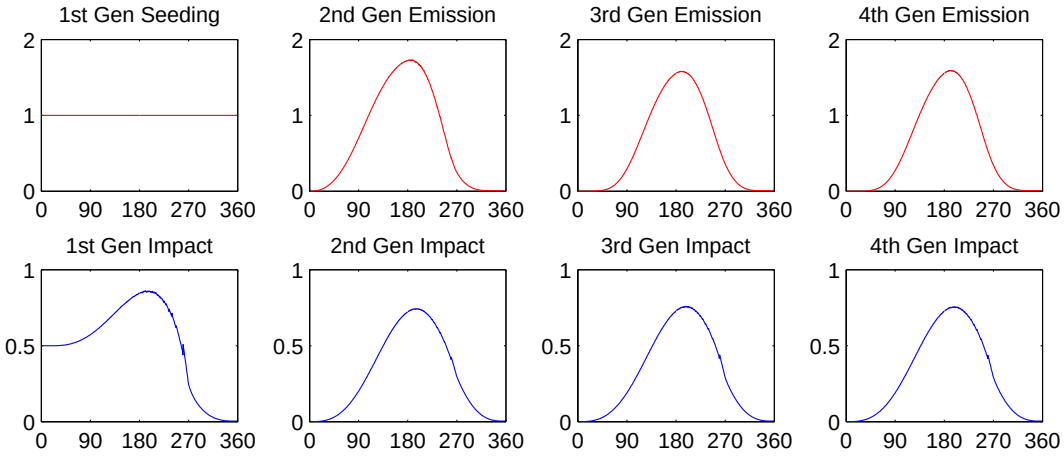

Fig. 6. The evolution of a uniform seeding distribution for successive generations of emission, transit, impact, and secondary emission. The short range returns are included in the analysis for $\alpha = 0$, and a Vaughan type model has been used.

CONCLUSIONS

A model has been devised that describes the impact phase statistics for non-resonant multipactor under the basic assumptions that electrons are reflected back to the emitting surface through some ponderomotive force, and that the flight time is long enough to ensure complete randomization of the arrival time of electrons into the region above the surface where they will impact the surface within one period. Since this model does not include the flight time of electrons, nor the emission velocity spread explicitly, the expressions for the impact probabilities are quite simple. A full analysis of the criterion for multipactor breakdown in these types of systems includes the nonlinear secondary emission yield function, and a comprehensive analysis is deemed too lengthy, and not included in this publication. We instead concentrated on calculating the impact distribution of electron number and velocity, along with the average impact speed, for some distributions over electron emission phases. This enabled us to draw some tentative conclusions. It appears that the statistical spread of electrons over impact phases can indeed be a strong loss source of electrons. The investigation of the extreme case when the emission speed of electrons is zero shows emission dynamics that are relatively simple, and the loss of electrons will be around half of the electron population for relevant distributions over electron emission phase. This result could explain the discrepancy between recent Monte Carlo simulations of the breakdown threshold in a two-wire system and the estimated threshold based on an average impact velocity approach. Future investigations will focus on using this method to calculate the multipactor breakdown threshold for values of the emission speed and the secondary emission yield curve, that are used in simulations, to test the ability of this model to reproduce the result from computer simulations.

REFERENCES

[1] J. R. M. Vaughan, “Multipactor”, IEEE Trans. Electron Dev., vol. 35, pp. 1172-1180, 1988.
[2] R. A. Kishek, Y. Y. Lau, L. K. Ang, A. Valfells and R. M. Gilgenbach, “Multipactor discharge on metal and dielectrics: Historical review and recent theories”, Phys. Plasmas, vol. 5, pp. 2120-2126, 1998.
[3] G. S. Luk’yanchikov, “Multiphase, uniform, secondary-emission microwave discharge at a solid surface”, Sov. Phys. Tech. Phys., vol. 19, pp. 1196-1199, 1975.
[4] A. Sazontov, M. Buyanova, V. Semenov, E. Rakova, N. Vdovicheva, D. Anderson, M. Lisak, J. Puech and L. Lapierre, “Effect of emission velocity spread of secondary electrons in two-sided multipactor”, Phys. Plasmas, vol. 12, 053102, 2005.
[5] R. Udiljak, D. Anderson, M. Lisak, V. E. Semenov, and J. Puech, “Multipactor in a coaxial transmission line, part I: analytical study”, Phys. Plasmas **14**, 033508, 2007.
[6] H. M. Wachowski, “Breakdown in waveguides due to the multipactor effect”, Report No. TDR-269(9990)-5, Aerospace Corp., El Segundo, California, 1964.
[7] N. K. Vdovicheva, A. G. Sazontov and V. E. Semenov, “Statistical theory of two-sided multipactor”, Radiophysics and Quantum Electronics, vol. 47, pp. 580-596, 2004.
[8] J. Rasch, D. Anderson, J. F. Johansson, M. Lisak, J. Puech, E. Rakova and V. E. Semenov, “Microwave Multipactor Breakdown Between Two Cylinders”, IEEE Trans. Plasma Sci., vol. 38, pp. 1997-2005, 2010.
[9] J. Rasch, V. E. Semenov, E. Rakova, D. Anderson, J. F. Johansson, M. Lisak and J. Puech, “Simulations of multipactor breakdown between two cylinders”, Accepted for publication in IEEE Trans. Plasma Sci.